Int. J. Electrochem. Sci., 8 **(2013)** 8848 - 8862

International Journal of
ELECTROCHEMICAL
SCIENCE
www.electrochemsci.org

Electrochemical Behavior of a Thio-Quinazoline Derivative Electrodeposited on a Glassy Carbon Electrode Modified with Multi-Wall Carbon Nanotubes: Application for Simultaneous Determination of Hydroxylamine and Nitrite

M. Mehdi Aghayizadeh[1], *Navid Nasirizadeh*[1,2,*], *S. Mansour Bidoki*[3], *M. Esmail Yazdanshenas*[1]

[1]Department of Textile Engineering, Yazd Branch, Islamic Azad University, Yazd, Iran
[2]Scientific Society of Nanotechnology, Yazd Branch, Islamic Azad University, Yazd, Iran
[3]Department of Textile, Yazd University, Yazd, Iran
[*]E-mail: nasirizadeh@yahoo.com

Received: 5 April 2013 / *Accepted:* 12 May 2013 / *Published:* 1 June 2013

In this paper, we report the characteristics of a modified electrode prepared by electrodeposition of anthio-quinazoline derivative on the multi-wall carbon nanotubes modified glassy carbon electrode (QMWCNT-GCE). The charge transfer coefficient, α, was calculated to be 0.43, and the charge transfer rate constant, k_s, was 12.6±0.3 s^{-1} in pH 7.0 between thio-quinazoline and MWCNT−GCE. The reactivity of this modified electrode for electrocatalytic oxidation of hydroxylamine was also examined. The results show that the sensitivity of hydroxylamine determination at a QMWCNT-GCE is remarkably improved and its overpotential is reduced when compared to MWCNT−GCE and QMGCE. By cyclic voltammetry, the kinetic parameters of electron transfer coefficient, α, the heterogeneous electron transfer rate constant, k′, and the exchange current, i_0, for the oxidation of hydroxylamine at the QMWCNT-GCE surface were calculated. Linear calibration curves were obtained for 3.0–69.8 μM and 69.8–915.2 μM of hydroxylamine at the modified electrode surface using an amperometric method. Also, the amperometric method exhibited the detection limit of 0.83 μM for hydroxylamine. The results indicate that the modified electrode is sensitive to hydroxylamine in the presence of nitrite (NO_2^-). Finally, the modified electrode was successfully applied for determination of hydroxylamine and NO_2^- in two water samples.

Keywords: Thio-quinazoline derivative, Multi-wall carbon nanotubes, Simultaneous determination, Hydroxylamine, Nitrite

1. INTRODUCTION

Hydroxylamine, NH_2OH, is one of the reducing agents widely used in industry and pharmacy. It is frequently used industrially in pharmaceutical intermediates and final drug substance synthesis,

nuclear fuel reprocessing, and semiconductor manufacturing [1]. NH_2OH is an intermediate in two important microbial processes of nitrogen cycle; it is formed during nitrification as well as anaerobic ammonium oxidation [2,3]. This compound is a well–known mutagen, moderately toxic and harmful to humans, animals, and even plants [4]. Moreover, some hydroxylamine derivatives constitute a great part of anticancer drugs [5]. In addition, hydroxylamine has been shown to inactivate or inhibit a number of cellular enzymes in vitro. It is also a skin irritant and sensitizer. Therefore, development of a sensitive analytical method for the determination of hydroxylamine at low levels is of great importance in industrial and environmental practices, clinical diagnostics, and biological processing [6]. So far, various methods such as chromatography [7,8] spectrophotometry [9,10] and polarography [11] have been reported for determination of hydroxylamine. In recent years, electrochemical techniques have been applied to determine hydroxylamine because they offer an opportunity for portable, rapid and cheap methodologies. At bare carbon electrodes, hydroxylamine cannot be oxidized. So, different chemically modified electrodes have been prepared to reduce the overvoltage and overcome the slow kinetics of many electrode processes [12–15]. We have already reported that coumestan derivative [16] rutin [5] indenedione derivative [17] ruthenium oxide [4] and oracet blue [18] modified electrodes could be successfully used to determine hydroxylamine.

In this report, we examine the electrochemical oxidation of hydroxylamine at thio-quinazoline derivative (see scheme 1 for structure) multi-wall carbon nanotubes modified glassy carbon electrode (QMWCNT-GCE). Also, the electrocatalytic oxidation of hydroxylamine at thio-quinazoline derivative modified GCE (QGCE), an MWCNT modified GCE (MWCNT−GCE), and an activated GCE (AGCE) was investigated. The results show that a combination of MWCNT and thio-quinazoline remarkably improves the sensitivity of hydroxylamine determination. Finally, the analytical application of QMWCNT–GCE is described as a voltammetric detector for hydroxylamine and nitrite simultaneous determination in two water samples.

2. EXPERIMENTAL

2.1. Apparatus and chemicals

Voltammetric measurements were carried out using an Autolab (Eco–Chemie, Ultrecht, and the Netherlands) potentiostat PGSTAT 30 equipped with GPES 4.9 equipped with a 663 VA stand three–electrode cell and a personal computer for data storage and processing. The working electrode was aQMWCNT–GCE, the auxiliary electrode consisted of a platinum wire, and the reference electrode was a saturated calomel electrode (SCE). pH measurements were done with a Metrohm model 827 pH/mV meter. All the measurements were made at room temperature.

An thio-quinazoline derivative, 2-[(4, 5-Dihydroxy-2-methylphenyl)thio]quinazoline-4(3H)-one (see Scheme 1 for the structure) was synthesized, purified, and characterized according to the procedure described before [19]. Hydroxylamine, sodium nitrite (NO_2^-), dimethyl formamide (DMF), and the other chemicals with analytical reagent grades were purchased from Merck Company. The multiwall carbon nanotubes (purity of N95%, diameter of 10–20 nm, and length of 5–20 μm) were obtained from Nanolab Inc. (Brighton, MA). An immobilizing solution of MWCNT was prepared by

introducing 5 mg of MWCNT into 5 ml of DMF. The phosphate buffer solutions (0.1M) were prepared with H_3PO_4, and the pH was adjusted with 2 M NaOH. All the aqueous solutions were prepared with doubly distilled water.

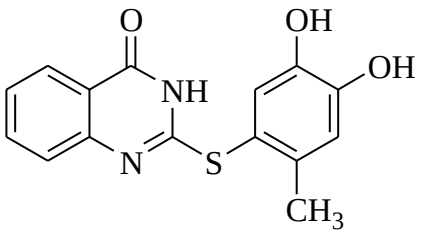

Scheme 1. Structure of the thio-quinazoline derivative

The glassy carbon electrode, GCE, was first polished mechanically with 0.05 μm alumina in water slurry using a polishing cloth and rinsed with doubly distilled water [20, 21]. For electrochemical activation of the glassy carbon electrode, it was immersed in a 0.1 M sodium bicarbonate solution and was activated by continuous potential cycling from −1.1 to 1.6 V at a sweep rate of 100 mV s^{-1}. To prepare thio-quinazoline modified GCE (QGCE), the activated GCE (AGCE) was rinsed with doubly distilled water and modified by cycling the potential between 40 mV and 300 mV at 20 mV s^{-1} in a 0.1 M phosphate buffer (pH 7.0). The fabrication of MWCNT and QMWCNT-GCE is described as follows. A 5 μl of MWCNT−DMF solution was placed directly onto the GCE surface and dried at room temperature to form a MWCNT film at the GCE surface and prepare an MWCNT–modified GCE (MWCNT−GCE). The QMWCNT-GCE was prepared by immersing the MWCNT−GCE in a 0.1 mM solution of thio-quinazoline in 0.1 M phosphate buffer (pH 7.0).It was then modified with the same procedure described for QGCE.

3. RESULTS AND DISCUSSION

3.1. Electrochemical characterization of QMWCNT–GCE

By a cyclic voltammetry technique, the electrochemical behavior of the modified electrodes was characterized. Fig. 1 indicates the cyclic voltammograms of QMWCNT-GCE in a 0.1 M phosphate buffer solution (pH 7.0) at various potential scan rates. As shown in Fig. 1A, the ratio of anodic to cathodic peak currents obtained at various scan rates is almost constant. Furthermore, the anodic and cathodic currents increase linearly with the scan rate in the whole worked scan rate potentials (Fig. 1A). For scan rate potentials at the range of 5 to 500 mV s^{-1}, the formal potential, $E^{0'}$, was almost independent of the potential scan rate. This is because of the facility of the charge transfer kinetics (Fig. 1B). The peak-to-peak potential separation ($\Delta E_p=E_{pa}-E_{pc}$) is about 42 mV for scan rate potentials below 200 mV s^{-1}. At high scan rates, the separation between peak potentials that increase with increased scan rates (Fig. 1B and C) indicates the limitation arising from the charge transfer kinetics.

Table 1. The surface charge transfer rate constant, k_s, and the charge transfer coefficient, α, for the electron transfer between the MWCNT-CCE and the Thio-quinazoline derivative at various pH.

pH	α	k_s/ s^{-1}
3.0	0.45	2.4± 0.06
5.0	0.45	3.9± 0.1
7.0	0.43	12.6± 0.25
9.0	0.48	12.5± 0.3

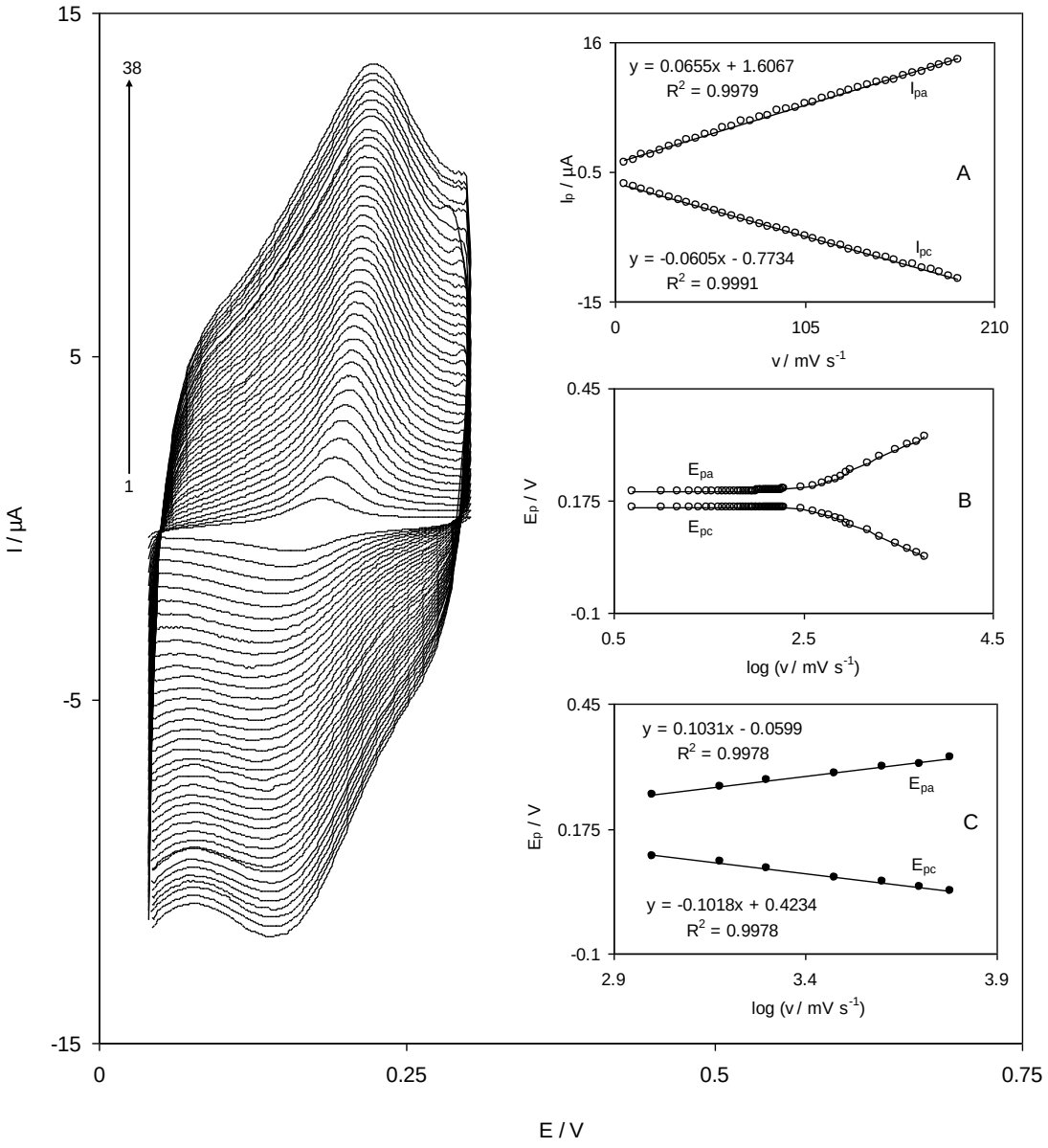

Figure 1. Cyclic voltammograms of the QMWCNT−GCE in 0.1 M phosphate buffer solution (pH 7.0) at different scan rates. The numbers 1–38 correspond to 5−190 mV s^{-1}. (A) Plots of anodic and cathodic peak currents vs. the scan rate. (B) Variation of the peak potentials vs. the logarithm of the scan rate. (C) Magnification of the plot inset B for high scan rates.

The results show that the values of the anodic and cathodic peak potentials were proportional to the logarithm of the scan rate for scan rates higher than 1000 mV s^{-1} (Fig. 1B and C). According to the method described by Laviron [22] the electron transfer coefficient, α, as well as the heterogeneous rate constant, k_s, for the charge transfer between the electrode and the surface confined redox couple can be evaluated from the slope and the intercept of variation of E_p versus log v at high scan rates respectively. Using the slope and the intercept of plots in Fig. 1, inset C, the values obtained for α and k_s were 0.43 and 12.6±0.3 s^{-1} at pH 7.0 respectively. The average values obtained for k_s are comparable to those reported for a modifier that has a hydroquinone moiety [23-26]. Also, the values of α and k_s were obtained at three pH levels because, in this case, these values were dependent on pH. The results are summarized in Table 1.

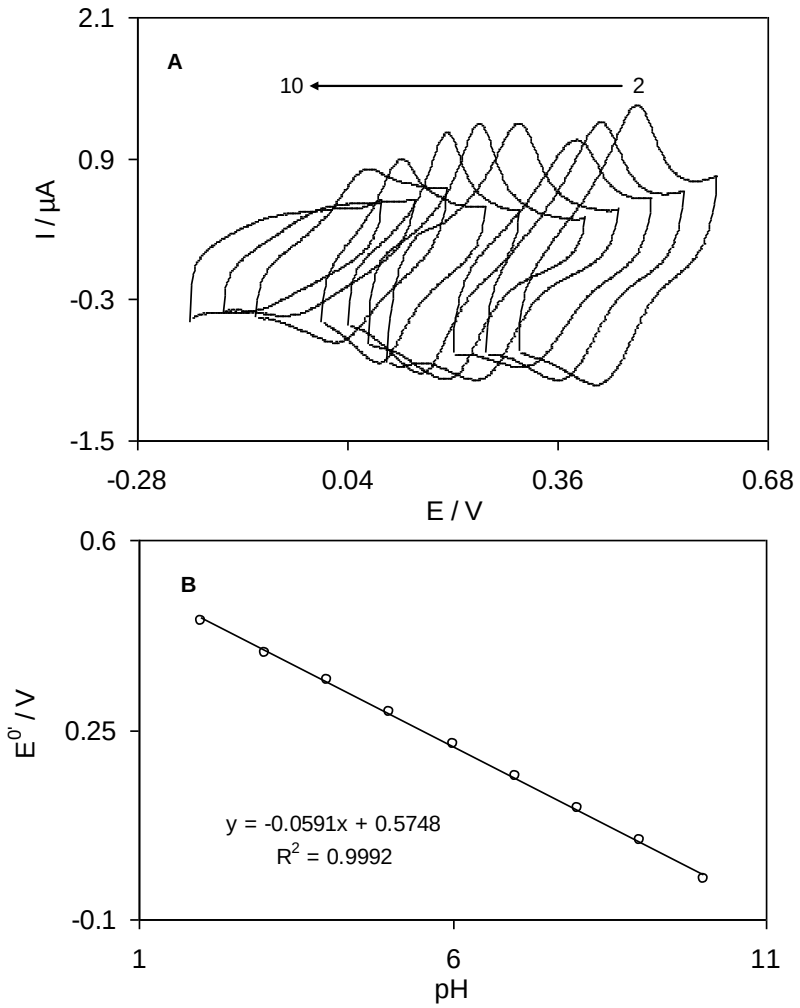

Figure 2. (A) Cyclic voltammograms QMWCNT−GCE at 20 mV s^{-1} in buffered pHs of 2.0, 3.0, 4.0, 5.0, 6.0, 7.0, 8.0, 9.0, and 10.0, respectively. (B) Plot of the formal potential, $E^{0'}$, vs. pH.

Since thio-quinazoline has an o–quinone moiety, it was anticipated that the redox response of the thio-quinazoline film would be pH-dependent. The influence of pH on the cyclic voltammograms at the QMWCNT–GCE surface in 0.1 M phosphate buffer solutions with different PHs at the scan rate

of 20 mV s^{-1} are shown in Fig. 2A. As it can be seen in Fig. 2B, the formal potential ($E^{0'}$) of QMWCNT–GCE is pH-dependent, and it shifts to a negative potential as pH is increased. The formal potential was obtained from the equation $E^{0'}=E_{pa}–\alpha\ (E_{pa}–E_{pc})$ [27]. The slope was found to be –59.1 mV pH^{-1} unit over a pH range from 2.0 to 10.0, which is very close to the Nernstian value of –59.2 mV pH^{-1} corresponding to a two–electron, two–proton electrochemical reaction.

3.2. Electrocatalytic oxidation of hydroxylamine at QMWCNT–GCE

The cyclic voltammograms at the QMWCNT–GCE, QGCE, MWCNT–GCE and AGCE were obtained in the absence and presence of 0.10 mM of hydroxylamine in a 0.1 M phosphate buffer solution (pH 7.0) to test the electrocatalytic activity of these modified electrodes (Fig. 3). Curves (a) and (b) of Fig. 3 indicate the cyclic voltammograms of QMWCNT–GCE in the absence (curve a) and the presence of 0.10 mM of hydroxylamine (curve b). As it is shown, there is an increase in the anodic peak current of QMWCNT–GCEox/QMWCNT–GCEred redox couple in the presence of hydroxylamine, whereas the reduction peak current has decreased. It reflects the efficiency of the catalytic reaction. This behavior confirms a very strong electrocatalytic effect for hydroxylamine at QMWCNT–GCE. As exhibited, the anodic peak potential for hydroxylamine oxidation at QMWCNT–GCE (curve b) is about 210 mV. However, at MWCNT–GCE (curve e) and activated GCE (curve f), the peak potentials are about 516 and 507 mV respectively. Therefore, the peak potential of hydroxylamine oxidation at QMWCNT-GCE (curve b) shifts by about 306, and 297 mV to more negative values compared with MWCNT−GCE (curve e) and AGCE (curve f) respectively. The electrocatalytic oxidation characteristics of hydroxylamine at various modified electrode surfaces at pH 7.0 are shown in Table 2. From Table 2, it is deduced that the best electrocatalytic effect for hydroxylamine oxidation is obtained at QMWCNT–GCE surface. To confirm this electrocatalytic effect, the dependence of the voltammetric response of QGCE on hydroxylamine concentration in pH=7.0 is depicted in the inset of Fig. 3. As it can be seen, the anodic peak current increasesbut the cathodic peak current decreases with an increasein the hydroxylamine concentration. This indicates the electrocatalytic oxidation of hydroxylamine at QGCE.

Table 2. Comparison the characteristics of hydroxylamine (0.1mM) on various electrode surfaces.

Name of electrode[a]	Oxidation peak potential (mV)	Oxidation peak current (μA)
AGCE	507	0.178
MWCNT−GCE	516	0.173
QGCE	210	0.103
QMWCNT−GCE	210	0.196

[a]AGCE: activated glassy carbon electrode, MWCNT−GCE: multi−wall carbon nanotubes modified glassy carbon electrode, QGCE: Thio-quinazoline modified glassy carbon electrode, QMWCNT−GCE: Thio-quinazoline multi−wall carbon nanotubes modified glassy carbon electrode.

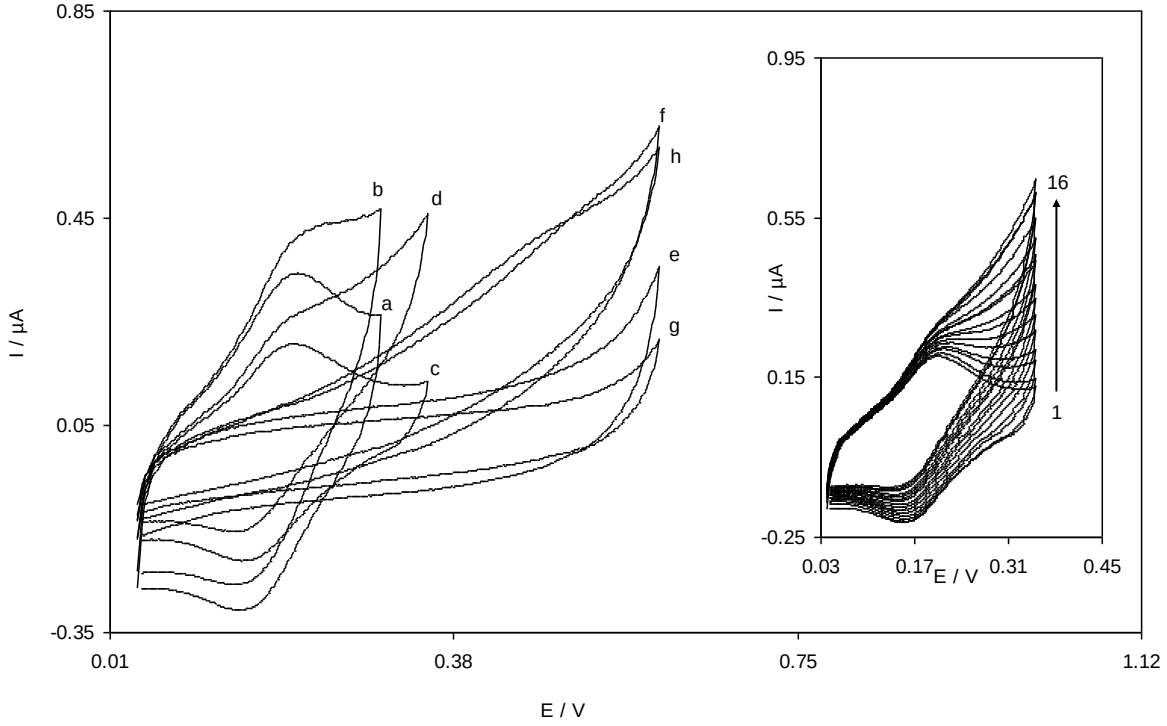

Figure 3. Cyclic voltammograms of QMWCNT−GCE in a 0.1 M phosphate buffer solution (pH 7.0) at scan rate 20 mV s^{-1} in (a) the absence and (b) the presence of 0.10 mM hydroxylamine,(c) as (a) for QGCE, (d), (e) and (f) as (b) for QGCE, MWCNT−GCE and AGCE respectively. Inset shows cyclic voltammograms of a QGCE in 0.1 M phosphate buffer solution containing various concentrations of hydroxylamine at 20 mV s^{-1}. The numbers of 1−16 correspond to different concentrations of 0.0–14.8 µM of hydroxylamine**.**

The cyclic voltammograms of a 0.10 mM hydroxylamine solution at different scan rate potentials are shown in Fig. 4A. The inset of Fig. 4A indicates that the plot of the catalytic peak current versus the square root of the scan rate potentials is linear, suggesting that the reaction is diffusion–limited. Based on these results, the catalytic reaction ($E_rC'_i$) describes the oxidation reaction of hydroxylamine by thio-quinazoline. For $E_rC'_i$ mechanisms, a theoretical model can be used to calculate the catalytic rate constant. Andrieux and Saveant [28] developed a theoretical model for such a mechanism and derived a relationship between the peak current and the concentration of the substrate for a case of a slow scan rate, v, and a large catalytic rate constant, k'. According to the theoretical model of Andrieux and Saveant and the useof Fig. 4A in their theoretical paper [28] the average value of k' was calculated to be $(6.25\pm0.15)\times10^{-4}$ cm s^{-1}. The number of electrons in the overall reaction can also be obtained from the slope of I_p versus $v^{1/2}$ plot (Fig. 4A, inset). According to the following equation for totally irreversible diffusion controlled processes [29-33]

$$I_p=3.01\times10^5 n[(1-\alpha)n_\alpha]^{1/2}AC_bD^{1/2}v^{1/2} \quad (1)$$

and considering $(1-\alpha)n_\alpha=0.6$ (see below), $D=7.33\times10^{-6}$ cm^2 s^{-1} (which is obtained by chronoampreometry) and A=0.0314 cm^2, it is estimated that the total number of electrons involved in the anodic oxidation of hydroxylamine is n=1.91≅2.

The linear sweep voltammograms of QMWCNT–GCE in a 0.1 M phosphate buffer solution (pH 7.0) containing 0.10 mM of hydroxylamine were obtained at different scan rates (Fig. 4B). In order to get information on the rate-determining step, the anodic Tafel plots were drawn (inset of Fig. 4B) using points of the Tafel region of the linear sweep voltammograms in Fig. 4B. The value of Tafel slope b= $(1-\alpha)n_\alpha$ F/2.3RT for hydroxylamine indicates that a one–electron transfer process is a rate–limiting step assuming an average charge transfer coefficient of α=0.40±0.01 for hydroxylamine. Moreover, the exchange current density, J_0, appears to be readily accessible from the intercept of the Tafel plots and geometric area [34]. The average value of the exchange current density, J_0, for hydroxylamine oxidation at the modified electrode surface was found to be 0.42±0.02 μA cm^{-2}.

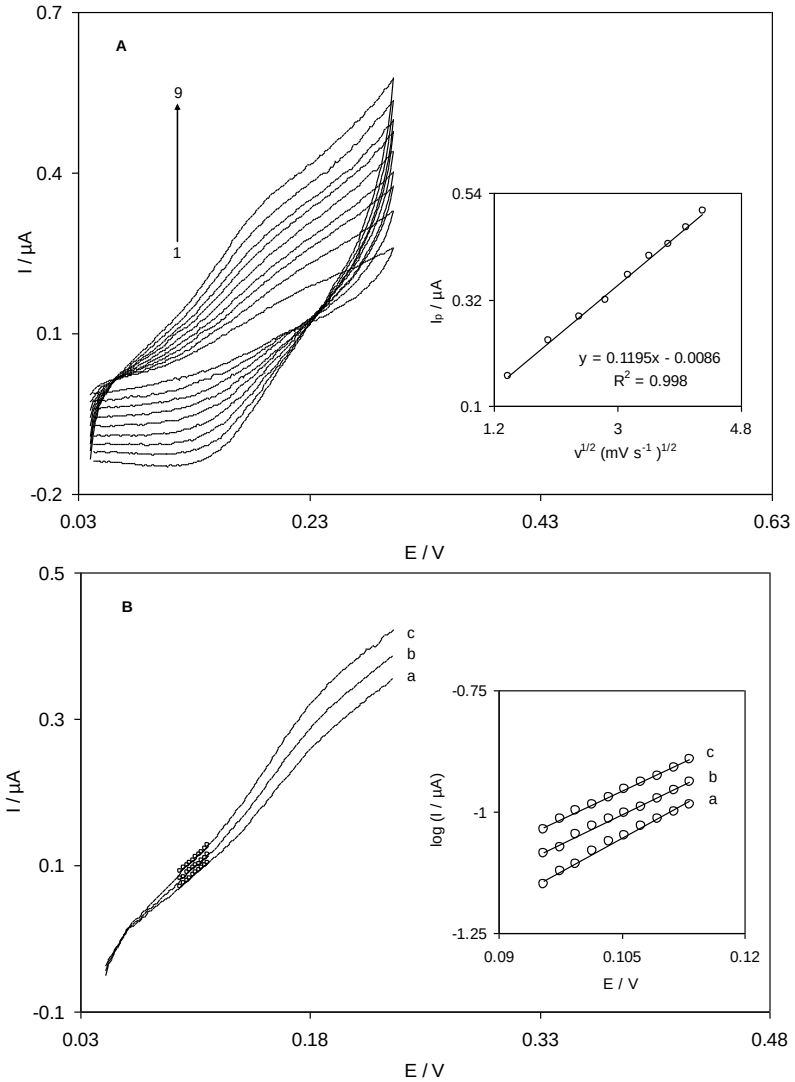

Figure 4. (A) Cyclic voltammograms of a QMWCNT−GCE in 0.1 M phosphate buffer solution (pH 7.0) containing 0.1 mM hydroxylamine. The numbers 1–9 correspond to scan rates of 2−18 mV s^{-1}. The inset shows the variation of the electrocatalytic peak current vs. the square root of scan rate. (B) Linear sweep voltammograms of QMWCNT−GCE in 0.1 M phosphate buffer (pH 7.0) containing 0.1 mM hydroxylamine at scan rates of 14 mV s^{-1}, 16 mV s^{-1}, and 18 mV s^{-1}. The points are the data used in the Tafel plots. The inset indicates the Tafel plots derived from linear sweep voltammograms.

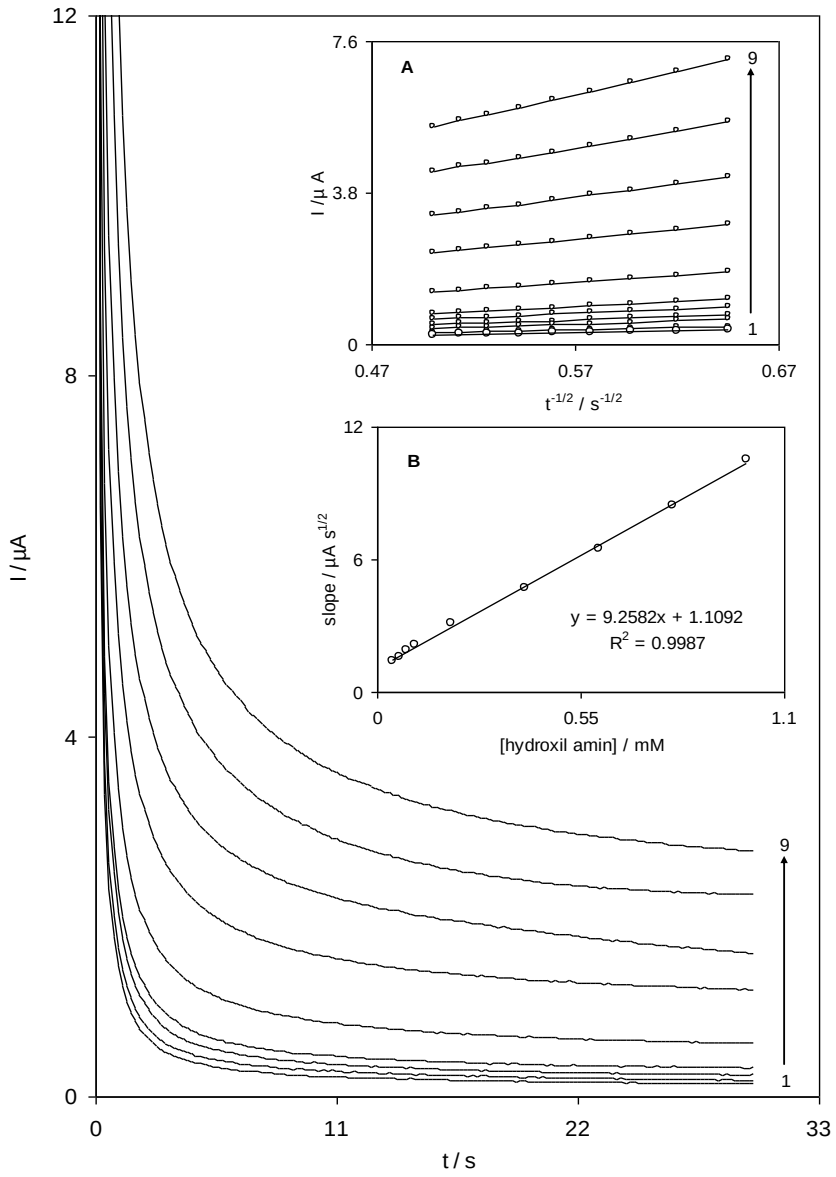

Figure 5. Chronoamperometric responses of QMWCNT−GCE in a 0.1 M phosphate buffer solution (pH 7.0) at potential step of 250 mV for different concentrations of 0.04–1.0mM hydroxylamine. (A) Plots of I vs. $t^{-1/2}$ obtained from the chronoamperograms. (B) Plot of the slopes of straight lines against the hydroxylamine concentrations.

In order to determinethe diffusion coefficient of hydroxylamine at QMWCNT–GCE,a chronoamperometry technique was used. Chronoamperograms were obtained by setting the working electrode potential at 220 mV for various concentrations of hydroxylamine (Fig. 5).

For an electroactive material with the diffusion coefficient D, the current response under diffusion control was described by Cottrell equation [35]

$$I=nFAD^{1/2}C_b/\pi^{1/2}t^{1/2} \quad (2)$$

Based on the Cottrell equation,the plot of I versus $t^{-1/2}$is linear, Fig. 5, inset A, shows the experimental plots I versus $t^{-1/2}$ for different concentrations of hydroxylamine. The slopes of the resulting straight lines are plotted versus the hydroxylamine concentration (Fig. 5, inset B), from

whose slope and using the Cottrell equation [34] we calculated a diffusion coefficient of 7.3×10^{-6} cm^2 s^{-1} for hydroxylamine.

3.3. Amperometric measurements

Amperometry was used to determine the linear ranges and the detection limits of hydroxylamine at QMWCNT–GCE. The use of amperometry was based on the fact that it has a much higher current sensitivity than cyclic voltammetry. Amperograms obtained for successive addition of hydroxylamine at potential steps of 250 mV and 750 mV are presented in Fig. 6A and B respectively. The insets a and b of Fig. 6A and B clearly indicate that the plot of the peak currents versus hydroxylamine concentration is constituted by two linear segments corresponding to two different ranges of 3.0–69.8 μM, 69.8–915.2 μM at the potential step of 250 mV and 1.4–82.4 μM, 82.4–907.5 μM at the potential step of 750 mV for hydroxylamine. According to the method mentioned in reference [35] the lower detection limit, C_m, was calculated using the equation $C_m=3s_{bl}/m$, where m is the slope of the calibration plot (0.0037 μA μM^{-1}) in the first linear range (3.0–69.8 μM), and s_{bl} is the standard deviation of the blank response which is obtained from 15 replicate measurements of the blank solution.

Through the data analysis, the detection limit of hydroxylamine was found to be 0.83 μM. The repeatability of QMWCNT–GCE was determined by 12 successive assays of a 0.83 μM hydroxylamine solution.

Table 3. Comparison some of the analytical parameters of hydroxylamine determination at different modified electrodes.

Modified electrode	Linear range (μM)	Sensitivity (μA μM)	Detection limit (μM)	Ref.
Fused TAA–AuNPs/MPTS/Au	0.0175–22000	0.0181	0.00039	[2]
RuON-GCE	4.0–33.8 33.8–78.3	–	0.45	[4]
RMWCNT–GCE	1.0–33.8 33.8–81.7	0.0288 0.025	1.0	[5]
AuNPs–SWCNTfilms	16–210	0.1659	0.72	[6]
ZnO nanofilm on to carbon nanotubes	0.4–19000	0.0075	0.12	[12]
NiCoHCF/GCE	20–200	0.00494	0.23	[14]
IMWCNT–CCE	1.0–10.0 10.0–100.0	0.1955 0.0841	0.8	[16]
CM–CCE	60–1000	–	10.75	[17]
OBMWCNT–GCE	4.0–102.4 102.4–5820.9	0.005 0.0004	0.7	[18]
Gold nanoparticle–polypyrole nanowire	1–500 500–18000	0.0639 0.0104	0.21	[36]
QMWCNT–GCE	3.0–69.8 69.8–915.2	0.0037 0.0016	0.83	This work

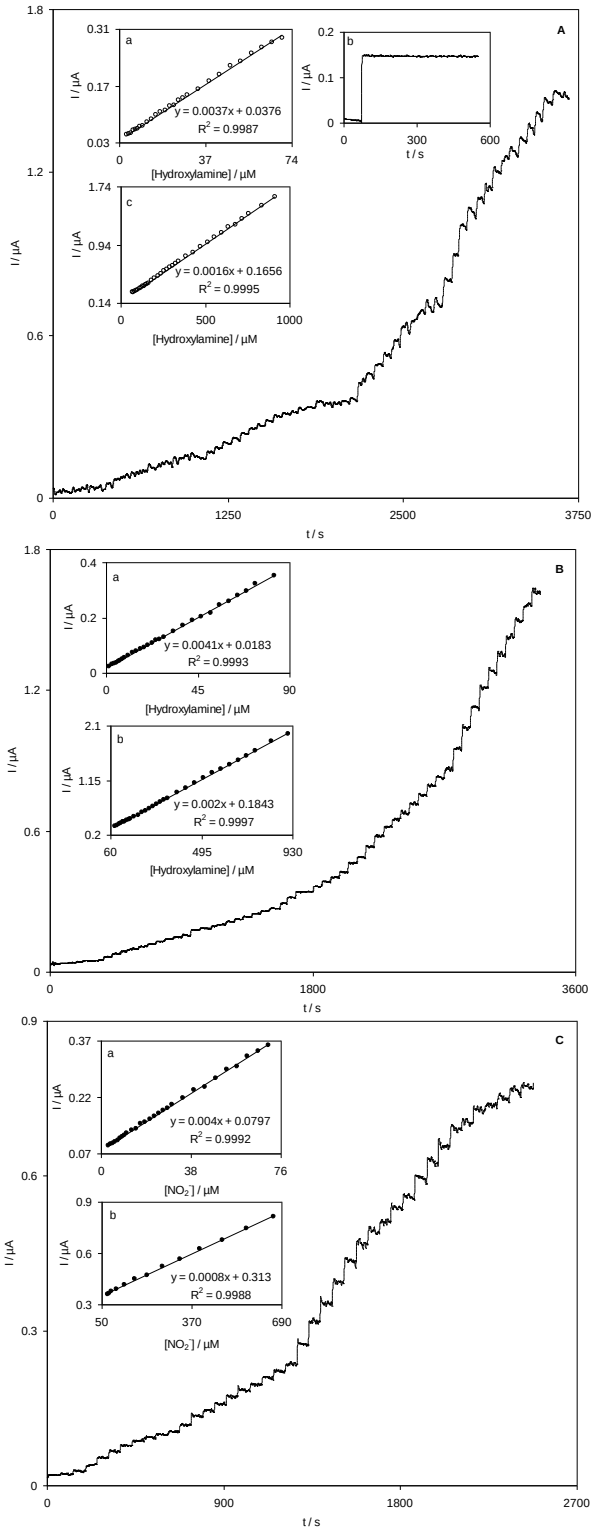

Figure 6. Amperometric responses at a rotating QMWCNT–GCE (rotation speed 2000 rpm) held at 250 mV (A) and 750 mV (B) in different concentrations of hydroxylamine. Insets a and b show variations of the amperometric currents vs. hydroxylamine concentrations in the ranges of 3.0–69.8 μM and 69.8–915.2 μM(A) and ranges of 1.4–82.4 μM and 82.4–907.5 μM. Inset c of (A) shows the stability of the response of QMWCNT–GCE to 30.0 μM hydroxylamine during 550 s. (C) Amperometric responses QMWCNT–GCE at 750 mV in different concentrations of NO_2^-.Insets a and b indicate variations of the amperometric currents vs. NO_2^-concentrations in the ranges of 3.0–70.6 μM and 70.6–660.8 μM.

The average amperometric current measured (μA) and the precision estimated in terms of the relative standard deviation (%R.S.D.) for 12 repeated measurements (n=12) of 15.0 μM hydroxylamine were 0.095±0.002 μA and 2.1% respectively. Also, the stability of QMWCNT–GCE in the presence of 30.0 μM hydroxylamine over a period of 550 secondsis shown in inset c of Fig. 6A. As it can be seen, no decrease was observed in the response current, and the amperometric current of hydroxylamine remained unchanged. This fact exhibits that there is no inhibition effect of hydroxylamine and its oxidation product for the modified electrode surface during this period of time. Fig. 6C indicates the amperograms which were recorded for QMWCNT–GCE (at a rotation speed of 2000 rpm), under conditions in which the potential was kept at 750 mV in a phosphate buffer solution (pH 7). Insets a and b of Fig. 6C clearly show that the plot of the peak currents versus NO_2^- concentration is made up of two linear segments corresponding to two different ranges of 3.0–70.6 μM and 70.6–660.8 μM of NO_2^-. Some of the electrocatalytic characteristics obtained in this work are compared with those previously reported by others (Table 3) [2, 4–6, 12, 14, 16–18, 36]. The data in Table 3 exhibit that the responses of the proposed modified electrode are, in some cases, superior as compared to those reported for the other modified electrodes.

In order to test its practical application, the modified electrode was used to determine hydroxylamine in the presence of NO_2^-. Figure 7A exhibits the amperometric response of QMWCNT–GCE for hydroxylamine in the presence of NO_2^- at the potential step of 220 mV. It is clear from Fig. 7A that addition of NO_2^- causes no change to the response current in amperometry. Moreover, the amperometric responses of hydroxylamine and NO_2were recorded under conditions where the potential was kept at 750 mV (Fig. 7B). It was noticed that when hydroxylamine and NO_2^-were added to the stirred buffer solution, the modified electrode responded rapidly to the substrate, and a well–defined current was produced.

In order to apply the proposed sensor for the determination of hydroxylamine and NO_2^- in real samples, it was tested by measuring hydroxylamine and NO_2^- in two water samples. At first, 5 mL of the water samples was diluted to 10 mL with a 0.1 M phosphate buffer solution (pH 7.0). Then, specificamounts of hydroxylamine and NO_2^- were added, and their recoveries were determined by the amperometric technique. The measurements were done using the calibration plots shown in the insets of Fig. 6.The results obtained are listed in Table 4. They show that RSD% and the recovery rates of the spiked hydroxylamine and NO_2^- were acceptable.

Table 4. Determination and recovery results of hydroxylamine (HA) and NO_2^- in water samples at a QMWCNT–GCE.

Samples		Added (μM)			Found (μM)			RSD %			Recovery %		
Tap water	HA	– 100	200	300	<D.L	99.3	201.7	303.2	2.2	2.7	2.1	1.8	99.3	100.8	101.1
	NO_2^-	– 150	300	450	<D.L	151.4	294.9	456.2	–	2.4	2.2	2.9	100.9	98.3	101.4
Drinking water	HA	– 75	150	225	<D.L	76.3	151.4	223.8	–	1.8	2.3	2.5	101.7	100.9	99.5
	NO_2^-	– 100	200	300	<D.L	98.9	202.5	302.6	2.3	2.9	1.9	2.3	98.9	101.2	100.9

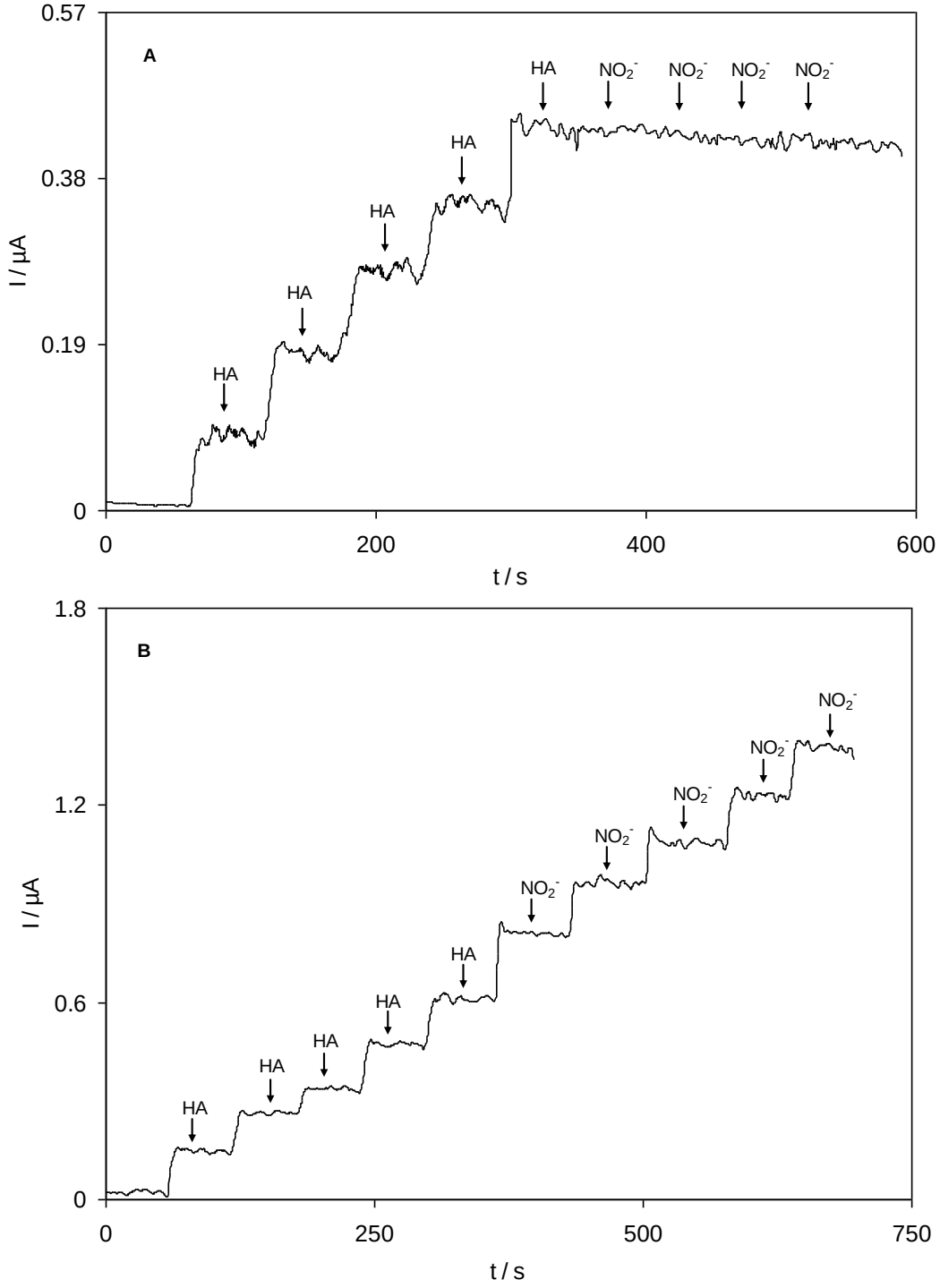

Figure 7. Amperometric response at a rotating QMWCNT–GCE (rotation speed 2000 rpm) kept in 250 mV (A) and 750 mV (B) in 10 ml phosphate buffer solution (0.1 M, pH 7.0) for successive addition of hydroxylamine and NO_2^-.

4. CONCLUSIONS

In this work, a QMWCNT–GCE was fabricated, and several methods were used to characterize this modified electrode. It was observed that hydroxylamine oxidation was catalyzed at the

QMWCNT–GCE surface, and its peak potential shifted to a less positive potential toward the MWCNT–GCE and AGCE. The standard heterogeneous rate constant, k', and the transfer coefficient, α, were calculated using cyclic voltammetry. The overall number of electrons involved in the catalytic oxidation of hydroxylamine was also calculated. In amperometric measurements, there appeared two linear calibration ranges for hydroxylamine and NO_2^-. Also, QMWCNT–GCE was used to determine hydroxylamine in the presence of NO_2^-. Finally, the modified electrode was applied for the determination of hydroxylamine and NO_2^- in water samples.

References

1. C. Zhang, G. Wang, M. Liu, Y. Feng, Z. Zhang and B. Fang, *Electrochim. Acta,* 55 (2010) 2835.
2. P. Kannan and S. Abraham, *Anal. Chim. Acta,* 663 (2010) 158.
3. J. Li and X. Lin, *Sens. Actuators B,* 126 (2007) 527.
4. H. R. Zare, S. H. Hashemi and A. Benvidi, *Anal. Chim. Acta*, 668 (2010) 182.
5. H. R. Zare, Z. Sobhani and M. Mazloum-Ardakani, *Sens. Actuators. B,* 126 (2007) 641.
6. M. P. Bui, X.H. Pham, K. N. Han, C. A. Li, E. K. Lee, H. Chang and G. H. Seong, *Electrochem. Commun.*, 12 (2010) 250.
7. Y. Seike, R. Fukumori, Y. Senga, H. Oka, K. Fujinaga and M. Okumura, *Anal. Sci*., 20 (2004) 139.
8. A. M. Prokai and R.K. Ravichandran *J. Chromatogr. A,* 667 (1994) 298.
9. A. Afkhami, T. Madrakian and A. Maleki, *Anal. Sci*., 22 (2006) 329.
10. E. Kavlentis, *Microchem. J.,* 37 (1988) 22.
11. D. R. Canterforf, *Anal. Chim. Acta*, 98 (1978) 205.
12. B. Fang, C. H. Zhang, G. F. Wang, M. Liu Y. H. Feng and Z. D. Zhang, *Electrochim. Acta*, 55 (2010) 2835.
13. A. Salimi and K. Abdi, *Talanta,* 63 (2004) 475.
14. L. H. Shi, T. Wu, P. He, D. Li, C.Y. Sun and J. H. Li, *Electroanalysis*, 17 (2005) 2190.
15. X. P. Cui, L. Hong and X. Q. Lin, *Anal. Sci*., 18 (2002) 543.
16. H. R. Zare and N. Nasirizadeh, *Electroanalysis*, 18 (2006) 507.
17. H. R. Zare, F. Chatraei and N. Nasirizadeh, *J. Brazil. Chem. Soc*., 21 (2010) 1977.
18. H. R. Zare and N. Nasirizadeh, *J. Brazil. Chem. Soc*., 23 (2012) 1070.
19. A. R. Fakhari, K. Hasheminasab, H. Ahmar and A. A. Alizadeh, *Synthesis*, 24 (2008) 3963
20. Y. Tang, C. Sun, X. Yang, X. Yang and R. F. Shen, *Int. J. Electrochem. Sci*., 8 (2013) 4194.
21. G. P. Keeley and M. E. G. Lyons, *Int. J. Electrochem. Sci.,* 4 (2009) 794.
22. E. Laviron, *J. Electroanal. Chem.,* 19 (1979) 19.
23. H. R. Zare, Z. Shekari, N. Nasirizadeh and A. A. Jafari, *Catal. Sci. Technol.,* 2 (2012) 2492.
24. N. Nasirizadeh, Z. Shekari, H. R. Zare, M. R. Shishehbore, A. R. Fakhari, and , H. Ahmar, *Biosens. Bioelectron.,* 41 (2013) 608.
25. N. Nasirizadeh, H. R. Zare, A. R. Fakhari, H. Ahmar, M. R. Ahmadzadeh and A. Naeimi, *J. Solid State Electrochem.,* 15 (2011) 683.
26. H. R. Zare, N. Nasirizadeh and M. Mazloum- Ardakani, *J. Electroanal. Chem.*, 577 (2005) 25.
27. H. Ju and C. Shen, *Electroanalysis,* 13 (2001) 789.
28. C. P. Andrieux and J. M. Saveant, *J. Electroanal. Chem.*, 93 (1978) 163.
29. S. Antoniadou , A. D. Jannakoudakis and E. Theodoridou, *Synth. Met,* 30 (1989) 295.
30. N. Nasirizadeh and H. R. Zare, *Talanta,* 80 (2009) 656.
31. H. R. Zare and N. Nasirizadeh, *Sens. Actuators. B,* 143 (2010) 666.
32. N. Nasirizadeh, Z. Shekari, H. R. Zare and S. Makarem, *Mater. Sci. Eng. C*, 33 (2013) 1491.
33. H. R. Zare and N. Nasirizadeh, *Int. J. Electrochem. Sci.*, 4 (2009) 1691.
34. A. J. Bard and L. R. Faulkner, Wiley. New York, (2001).

35. D. A. Skoog, F. J. Holler and T. A. Nieman, fifthed., Harcourt Brace, Philadelphia, (1998).
36. J. Zhang, J. Tse, Y. H. Pietro and W. J. Lever, *J. Electroanal. Chem.*, 406 (1996) 203.